Molecular Crystals and Liquid Crystals
Publication details, including instructions for authors and subscription information:
http://www.tandfonline.com/loi/gmcl20

Analysis of Mesogenic Characteristics of 6-Chloro-benzothiazol-2-yl-(4-hexadecyloxyphenyl) Diazene—A Smectic Liquid Crystal

M. Roychoudhury [a], Pankaj Kumar Gaurav [a], Rajiv Manohar [b] & A. K. Prajapati [c]

[a] Department of Physics, D.D.U. Gorakhpur University, Gorakhpur (U.P.), India

[b] Department of Physics, University of Lucknow, Lucknow, India

[c] Department of Applied Chemistry, Faculty of Technology and Engineering, M.S. University of Baroda, Vadodara, India

Version of record first published: 08 Apr 2011

To cite this article: M. Roychoudhury, Pankaj Kumar Gaurav, Rajiv Manohar & A. K. Prajapati (2011): Analysis of Mesogenic Characteristics of 6-Chloro-benzothiazol-2-yl-(4-hexadecyloxyphenyl) Diazene—A Smectic Liquid Crystal, Molecular Crystals and Liquid Crystals, 537:1, 3-21

To link to this article: http://dx.doi.org/10.1080/15421406.2011.556394

Mol. Cryst. Liq. Cryst., Vol. 537: pp. 3–21, 2011

ISSN: 1542-1406 print/1563-5287 online
DOI: 10.1080/15421406.2011.556394

Taylor & Francis
Taylor & Francis Group

Analysis of Mesogenic Characteristics of 6-Chloro-benzothiazol-2-yl-(4-hexadecyloxyphenyl) Diazene—A Smectic Liquid Crystal

M. ROYCHOUDHURY,[1] PANKAJ KUMAR GAURAV,[1] RAJIV MANOHAR,[2] AND A. K. PRAJAPATI[3]

[1]Department of Physics, D.D.U. Gorakhpur University, Gorakhpur (U.P.), India
[2]Department of Physics, University of Lucknow, Lucknow, India
[3]Department of Applied Chemistry, Faculty of Technology and Engineering, M.S. University of Baroda, Vadodara, India

*Measurements of dielectric constant and dielectric loss at various frequencies have been carried out on the title compound for the entire smectic range of temperature. Dielectric strength, distribution parameter, and activation energy as evaluated from the experimental data are reported in the article. To obtain a deeper insight, the intermolecular interaction between a pair of 6CB4HPD molecules has been analyzed using quantum mechanically optimized molecular geometry and electronic structure with the help of the Gaussian 03 program (Gaussian, Inc., Wallingford, CT) along with B3LYP/6-31G** basis sets. An attempt has been made to correlate the molecular structure, relative energy, and configuration of various interacting pairs and the observed experimental findings.*

Keywords 6CB4HPD; dielectric permittivity; Gaussian; intermolecular interaction; smectic A

Introduction

Ever since liquid crystals were discovered, due to their peculiar properties, interest in determining their molecular and electronic structures has never decreased [1,2]. Efforts are also being made to evaluate molecular parameters from dielectric measurements [3]. Further development of biological and technological application of liquid crystals depends on the success of a more fundamental understanding of the relation between molecular structure and corresponding bulk properties such as transition temperature or dielectric anisotropy. These are dependent not only on the electronic properties of individual molecules but also on the properties that are determined by the interaction between the molecules [4–6].

Address correspondence to M. Roychoudhury, Department of Physics, D.D.U. Gorakhpur University, Gorakhpur 273009, India. E-mail: mrcgkpu@rediffmail.com

The compound chosen for the present study, 6-chloro-benzothiazole-2yl-(4-hexadecyloxy-phenyl) diazene, exhibits a phase transition sequence as follows:

$$\text{Crystal} \xrightarrow{97^{\circ}\text{C}} \text{Sm A} \xrightarrow{176^{\circ}\text{C}} \text{Isotropic}$$

In the present work, the variation of dielectric constant and dielectric loss was studied for the entire smectic range of temperature. Further, the electronic structure of the molecule was determined using a quantum mechanical method. Thereafter, various possible modes of intermolecular interaction were studied in order to find out the molecular preferences during the transition from a crystalline phase to an isotropic liquid phase.

Method

The quantum mechanical framework adopted for the present work is described below. The procedure is known as the Rayleigh-Schrodinger perturbation approach for long-range interactions.

Using Born-Oppenheimer approximation [7], nuclear motion is separable from electronic motion. The complete Hamiltonian operator corresponding to electronic motion of a pair of molecules can be expressed as:

$$H = H^{(a)} + H^{(b)} + H' \tag{1}$$

where $H^{(a)}$ and $H^{(b)}$ denote the Hamiltonian operators corresponding to free molecules a and b. Keeping the contribution confined to Coulombic interactions

$$H' = \sum q_i^{(a)} q_j^{(b)} (R_{ij})^{-1} \tag{2}$$

where $q_i^{(a)}$, $q_j^{(b)}$ are the charges on molecules a and b, respectively, and R_{ij} is the distance between them.

A general theory of long-range intermolecular forces is obtained by treating H′ as a perturbation to $H^{(a)}$ and $H^{(b)}$. The unperturbed wave functions are the eigenfunctions of $H^{(a)}$ and $H^{(b)}$ and are therefore simple products of the wave functions of the free molecules a and b. The perturbed wave function may now be expressed in terms of these unperturbed states by using standard quantum mechanical perturbation theory [8–10] and is

$$|\psi_{m_a m_b}\rangle = \left| m_a m_b \rangle + \sum_{p_a p_b}{}' \frac{\langle p_a p_b | H' | m_a m_b \rangle}{W_{m_a} + W_{m_b} - W_{p_a} - W_{p_b}} \right| p_a p_b \rangle + \cdots \tag{3}$$

where the symbol Σ' denotes a sum over the complete set of unperturbed states p_a, p_b except the initial state, m_a, m_b. The first-order perturbation wave function therefore consists of the addition to the unperturbed function $|m_a m_b\rangle$ of a small amount of all those other unperturbed states of the system that are mixed with $|m_a m_b\rangle$ by the perturbation H'. The extent of the admixture is proportional to the off-diagonal matrix element $\langle p_a p_b | H' | m_a m_b \rangle$ and inversely to the difference in the energies of the unperturbed states, $[(W_{m_a} + W_{m_b}) - (W_{p_a} + W_{p_b})]$. The unperturbed states are assumed

to be normalized. The energy of the pair of molecules in the perturbed state, $\psi_{m_a m_b}$, is

$$W_{m_a m_b} = \frac{\langle \psi_{m_a m_b} | H | \psi_{m_a m_b} \rangle}{\langle \psi_{m_a m_b} | \psi_{m_a m_b} \rangle} = W_{m_a} + W_{m_b} + \langle m_a m_b | H' | m_a m_b \rangle - \sum_{p_a, p_b}{}' \frac{|\langle p_a p_b | H' | m_a m_b \rangle|^2}{W_{p_a} + W_{p_b} - W_{m_a} - W_{m_b}} + \cdots \quad (4)$$

The first-order energy $\langle m_a m_b | H' | m_a m_b \rangle$ is the unperturbed expectation value of the perturbation H' and is the electrostatic interaction energy $E_{\text{electrostatic}}$. The second-order energy may be separated into two distinct contributions. The first, which is the induction energy $E_{\text{induction}}$, consists of all those terms in which either $p_b = m_b$ with $p_a \neq m_a$ or $p_a = m_a$ with $p_b \neq m_b$. The other contribution is $E_{\text{dispersion}}$, which is composed of the remaining terms where $p_a \neq m_a$ and $p_b \neq m_b$. The induction energy is therefore the sum of two parts

$$E_{\text{induction}} = E^{(a)}_{\text{induction}} + E^{(b)}_{\text{induction}} \quad (5)$$

where

$$E^{(\text{a})}_{\text{induction}} = - \sum_{p_a \neq m_a} \frac{|\langle p_a m_b | H' | m_a m_b \rangle|^2}{W_{p_a} - W_{m_a}}$$

and

$$E^{(\text{b})}_{\text{induction}} = - \sum_{p_b \neq m_b} \frac{|\langle m_a p_b | H' | m_a m_b \rangle|^2}{W_{p_b} - W_{m_b}}$$

Similarly,

$$E_{\text{dispersion}} = - \sum_{p_a \neq m_a, p_b \neq m_b} \frac{|\langle p_a p_b | H' | m_a m_b \rangle|^2}{W_{p_a} + W_{p_b} - W_{m_a} - W_{m_b}} \quad (6)$$

If the initial state $|m_a m_b\rangle$ is degenerate, then it is necessary to choose, as the zeroth-order state, the mixture of the degenerate states that diagonalizes the Hamiltonian H. If degeneracy is m-fold, there are m such independent states; if one of them is $|m'_a m'_b\rangle$, the corresponding energy to the first order in H' is

$$\langle m'_a m'_b | H^{(a)} + H^{(b)} + H' | m'_a m'_b \rangle = W_{m_a} + W_{m_b} + E_{\text{electrostatic}} + E_{\text{resonance}} \quad (7)$$

The second-order energy is the sum over all unperturbed states $|p_a p_b\rangle$ that are not degenerate with $|m_a m_b\rangle$ and is again the sum of induction and dispersion energy terms.

The various energy quantities may be successfully related with the properties of the free molecules; that is, the charge, dipole moment, quadrupole moment, and polarizabilities for which a detailed mathematical framework has been discussed by Buckingham [11].

A detailed computational scheme has been provided by Claverie [12] suitable for evaluation of the interaction energy of large interacting systems of whatever complexity. The simplified formulas prescribed by Claverie are as follows.

Simplified Formula

The total intermolecular interaction energy E_{tot} between any two molecules may be expressed as the sum of various contributing terms. Accordingly,

$$E_{\text{tot}} = E_{\text{el}} + E_{\text{ind}} + E_{\text{disp}} + E_{\text{rep}} \tag{8}$$

where E_{el}, E_{ind}, E_{disp}, and E_{rep} represent the electrostatic, induction, dispersion, and repulsion components, respectively.

Electrostatic Energy. The molecular charge distribution is expressed as a set of atomic charges (q) (referred to as *monopoles*) and atomic dipoles (μ) that can be obtained using any all valence electron molecular orbital method. According to a multicentered multipole expansion method, the electrostatic energy may be expressed as the sum of the individual terms between atomic multipoles as.

$$E_{\text{el}} = E_{\text{QQ}} + E_{\text{QM}} + E_{\text{MM}} + \cdots \tag{9}$$

where E_{QQ}, E_{QM}, E_{MM}, etc., are the monopole–monopole, monopole–dipole, dipole–dipole terms, etc., respectively. In general, the first three terms have been found to be adequate for most molecular systems. The monopole–monopole term E_{QQ} is given by

$$E_{\text{QQ}} = C \sum_{i,j} \frac{q_i q_j}{r_{ij}} \tag{10}$$

where q_i, q_j are the monopoles on each atomic center of the interacting molecules i and j, r_{ij} is the interatomic distance, and C takes care of the units. If the charges are expressed in electronic charge unit and distances r_{ij} in angstrom, the value of $C = 331.934$ expresses the energy in kcal/mol. The monopole–dipole energy term may be expressed as

$$E_{\text{QM}} = C \sum_{i,j} q_i \vec{\mu}_j \cdot \frac{\vec{r}}{r^3} \tag{11}$$

and the dipole–dipole interacting term is given by

$$E_{\text{MM}} = \frac{C}{r^3} \sum_{i,j} \left[\vec{\mu}_i \vec{\mu}_j - 3 \left(\vec{\mu}_i \cdot \frac{\vec{r}}{r} \right) \left(\vec{\mu}_j \cdot \frac{\vec{r}}{r} \right) \right] \tag{12}$$

where $\vec{\mu_i}$, $\vec{\mu_j}$ represent the atomic dipoles and the subscript r used in the above equation has been removed without any change in its meaning.

Polarization Energy. The polarization energy, sometimes called the *induction energy*, of a molecule say (s) is obtained as sum of induced polarization for the various

bonds involved:

$$E_{\text{ind}}^{(S)} = C\left(-\frac{1}{2}\right)\sum_{u}{}^{(S)}\vec{\varepsilon}_u^{[S]}\overline{\overline{A}}_u^{(S)}\vec{\varepsilon}_u^{[S]} \tag{13}$$

where $\overline{\overline{A}}_u$ is the polarizability tensor of the bond u and $\vec{\varepsilon}_u^{[S]}$ is the electric field created at this bond by the surrounding molecules other than (S). If the molecular charge distribution is represented by the atomic net charges, it is found that

$$\vec{\varepsilon}_u^{[S]} = \sum_{t\neq S}\sum_{\lambda}{}^{(t)}q_\lambda^{(t)}\cdot\frac{\vec{R}_{\lambda u}}{R_{\lambda u}^3} \tag{14}$$

where $\vec{R}_{\lambda u}$ is the vector joining the atom λ in molecule (t) to the center of the polarizable charge on the bond u of the molecule (S).

The polarizability tensor of the bond μ of the molecules (s), A_u, is of the diagonal form. In case the X-axis of the local coordinate system is directed along the bond u, the polarizability may be expressed as

$$A = \begin{bmatrix} A_L & 0 & 0 \\ 0 & A_T & 0 \\ 0 & 0 & A_V \end{bmatrix} \tag{15}$$

where A_L, A_T, and A_V are principal polarizabilities of the bond. For most cases $A_T = A_V$, and when they are not equal, A_T and A_V are replaced by their average values. The values of bond polarizabilities may be obtained from the experimental data for polarizabilities as done by the several workers [13,14]. The values for some of the bond polarizabilities not available in the literature may be evaluated from polarizabilities of similar molecules. Huron and Claverie [15] thus obtained the values for O-H (from CH_3OH) of $A_L = 0.61\text{A}^3$, $A_T = 0.76\text{A}^3$ and for N-O of the nitro group - NO_2, they used $A_L = 2.48\text{A3}$, $A_T = 0.62\text{A}^3$. The recommended value for C=N is $A_L = 2.43\text{A}^3$, $A_T = 1.00\text{A}^3$ [12].

Dispersive and Short-Range Repulsion Energies. These two terms have been traditionally considered together as has been done in the semi-empirical derivations of the Lennard-Jones or Buckingham-type cases. As mentioned earlier, Kitaigorodskii adopted the 6-exp potential and later modified the parameters to suit all types of molecular systems. Accordingly,

$$E_{\text{disp}} + E_{\text{rep}} = \sum_{\lambda}{}^{(1)}\sum_{\nu}{}^{(2)}E(\lambda,\nu) \tag{16}$$

where

$$E(\lambda,\nu) = K_\lambda K_\nu\left(\frac{-A}{z^6} + Be^{-\gamma z}\right)$$

and

$$z = \frac{R_{\lambda\nu}}{R_{\lambda\nu}^0}, \quad R_{\lambda\nu}^0 = \sqrt{(2R_\lambda^w)(2R_\nu^w)}$$

where R_λ^w and R_ν^w are the van der Waals radii of atoms λ and ν, respectively. The parameters A, B, and γ are not dependent on the atomic species: this necessary dependence is brought about by $R_{\lambda\nu}^w$ and by the factors K_λ and K_ν, which allow the energy minima to have different values according to the atomic species involved [16,17]. The numerical values of these parameters, used by most authors are, $A = 0.214$, $B = 0.214$, and $\gamma = 12.35$.

As a further refinement [18], the dependence of the repulsion term on the residual charge has been taken into account by multiplying it by two factors that are functions of the charges on the two atoms concerned. Thus, if q_λ and q_ν are the net atomic charges and N_λ and N_ν the atomic number, the actual electron populations are $(N_\lambda - q_\lambda)$ and $(N_\nu - q_\nu)$ and atom-atom repulsion term [19] is $E_{\text{rep}}(\lambda, \nu)$.

Thus, the modified short-range energy is:

$$E_{\text{rep}}^{\text{modified}}(\lambda, \nu) = \left(1 - \frac{q_\lambda}{N_\lambda}\right)\left(1 - \frac{q_\nu}{N_\nu}\right) E_{\text{rep}}(\lambda, \nu) \tag{17}$$

where

$$E_{\text{rep}}(\lambda, \nu) = K_\lambda K_\nu B \exp(-\gamma R_{\lambda\nu}/R_{\lambda\nu}^0).$$

This correction is usually small in most of the cases, but it becomes significant for hydrogen atoms with a non negligible (positive) charge; for example, those bonded with oxygen and/or nitrogen atoms because $N_H = 1$.

The formalism described above has the additional advantage that it represents hydrogen bonding interactions only by introducing some minor modification in the repulsion term. The orientation of the repulsion term is modified by decreasing B and increasing γ below a certain prescribed distance. The details of the hydrogen bond representation have been extensively discussed by Claverie [12].

The electronic structure of the compound was determined after geometrical optimization of the structure using the Gaussian 03 program [20] with B3LYP/6-31G** basis sets. The structure was fully optimized without any constraints and checked for imaginary frequencies. Intermolecular interaction energy between a pair of molecules was evaluated for the following interacting conditions (a) stacking, (b) planar, and (c) terminal interaction on both sides of the molecule. This method was applied in the literature [21–23] to analyze liquid-crystalline behavior of various molecules. Although the earlier results were promising, they were often subjected to criticism due to the unoptimized geometry and electronic structure calculated by employing an approximate method (CNDO/2). In the present work, computations have been carried out on the basis of fully optimized geometry and state-of-the-art charge distribution.

It is important to change the configuration continuously at short intervals and compute energy at each point so that the variation of energy can be studied with respect to the configurational changes. A global search of minimum energy configuration is difficult and time consuming because it involves many unfavorable configurations that could be avoided by choosing a suitable path for minimization. Because the systems under study are mostly of a long and flat molecular structure, the interaction scheme has been divided into the following categories as shown in Figure 1:

(I) Stacking interaction
(II) In-plane interaction
(III) Terminal interaction

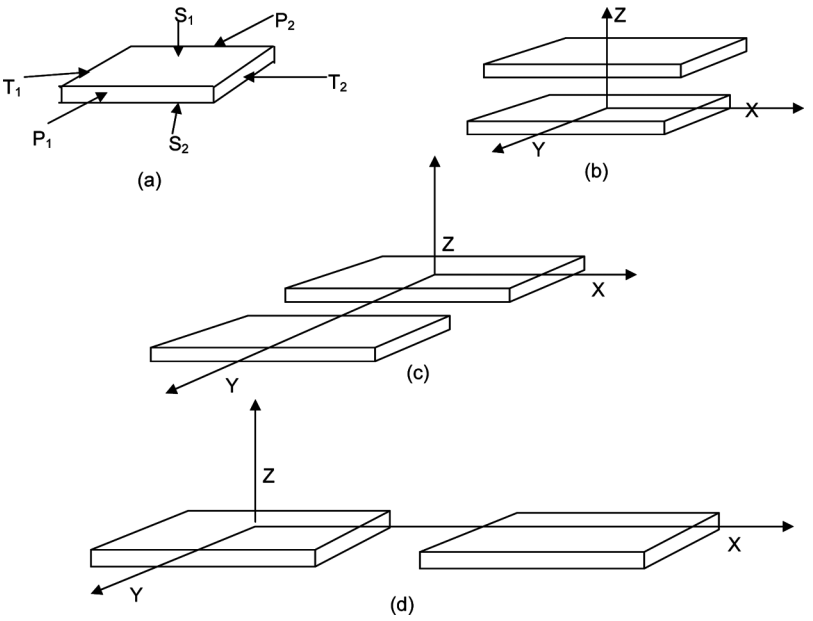

Figure 1. The three modes of interactions of a molecular pair: (a) sides, faces, and terminals of a molecule; (b) stacking interaction; (c) in-plane interaction; and (d) terminal interaction.

Results and Discussion

Experimental

The compound 6CB4HPD was synthesized in pure form at M.S. University, Baroda, India. Dielectric measurements were carried out on an Hewlett-Packard-4194A computer-controlled impedance/gain phase analyzer. The real and imaginary parts of the sample were obtained using the following relations (18) and (19):

$$\varepsilon' = \{(C_m - C_0)/C_l\} + 1 \tag{18}$$

$$\varepsilon'' = (G_m - G_0)/2\pi f C_l \tag{19}$$

where C_m and G_m are the capacitance and conductance of the cell filled with sample, C_0 and G_0 are the capacitance and conductance of the cell without sample, and C_l is the live capacitance. The chemical structure of the studied compound 6CB4HPD is shown in Figure 2.

The variation of dielectric constant and dielectric loss with respect to frequency for the temperature range 110°C to 170°C at intervals of 10°C is presented in Figures 3 and 4, respectively.

It may be observed that both the dielectric constant and loss curves exhibit a shift towards, higher frequency with increase in temperature. The peak of dielectric loss appears between 1 and 10 KHz for different temperatures.

The corresponding Cole-Cole plot for temperatures 110°C–160°C is presented in Figure 5. Not much dispersion was observed in the Cole-Cole plot, hence, they are shown separately for each temperature.

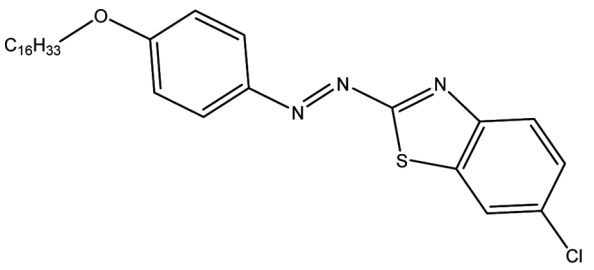

Figure 2. Chemical structure of 6-chloro-benzothiazole-2-yl-(4-hexadecyloxy-phenyl) diazene.

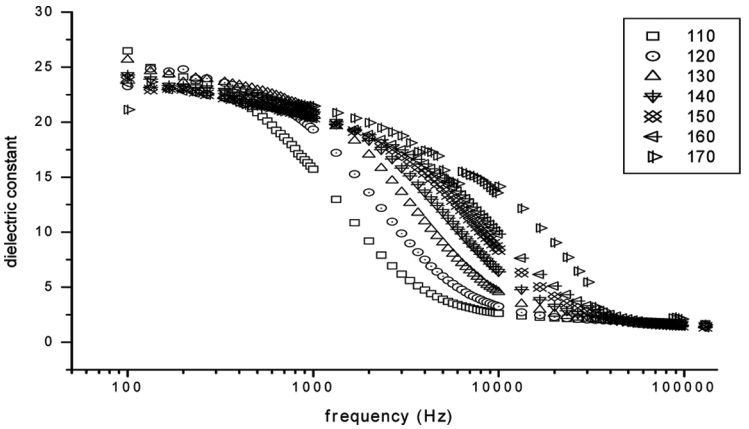

Figure 3. Behavior of dielectric constant with variation of frequency in the smectic phase region 110°C to 170°C.

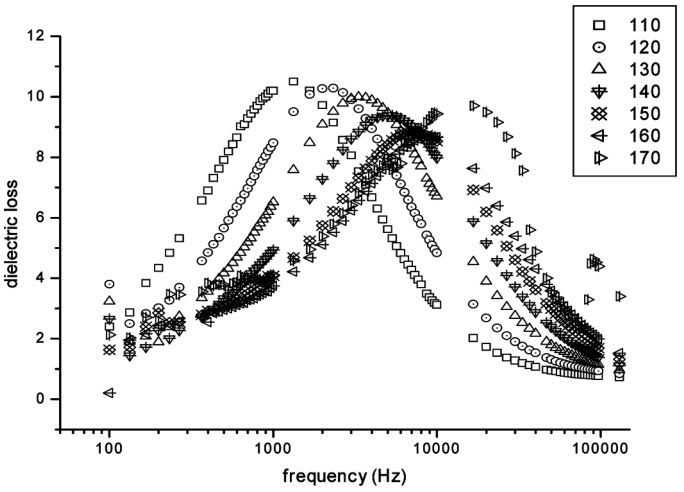

Figure 4. Behavior of dielectric loss with variation of frequency in the smectic phase region 110°C to 170°C.

Variation of dielectric strength ($\varepsilon_0 - \varepsilon_\infty$) with temperature is shown in Figure 6 and that of the distribution parameter (α) is presented in Figure 7.

Variation of frequency ($\log_{10}$) with 10^3/T yields a straight line. This linear nature follows an Arrhenius equation and is shown in Figure 8.

$$Fc = Fo \ \exp(-E/KT) \tag{20}$$

The activation energy E is calculated from the slope of this plot in smectic A phase as

$$E = 4.19 \times 10^{-24} \text{ J/mol}$$

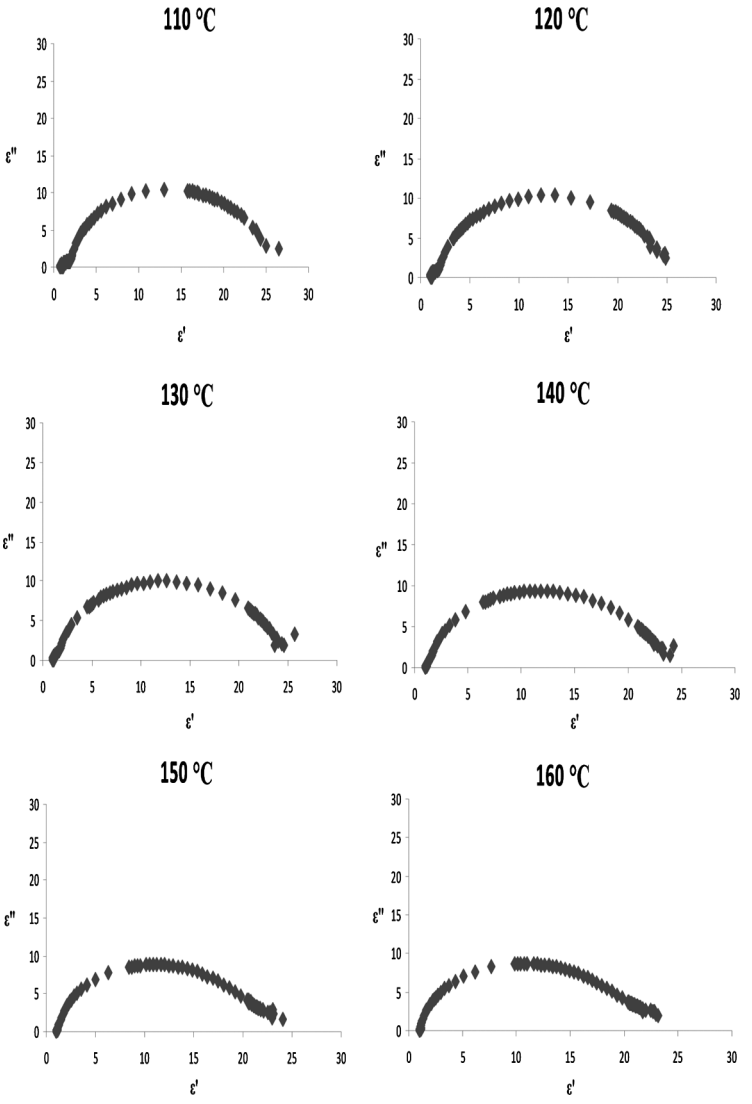

Figure 5. Cole-Cole plot dielectric loss (ε'') versus dielectric constant (ε') at different temperatures.

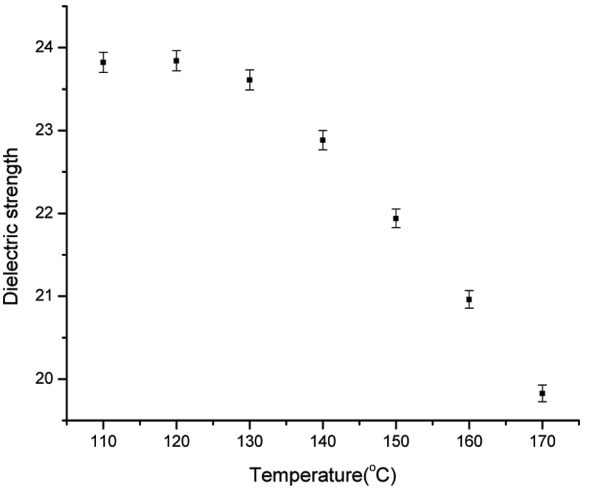

Figure 6. Variation of dielectric strength with temperature.

Computational

Figure 9 shows the optimized geometry of the molecule obtained using Gaussian 03 with the numbering scheme used in this work.

It may be observed that the benzothiazole and phenyl rings are almost in the same plane with the alkoxy tail, although the tail is slightly bent. Table 1 lists the optimized coordinates of various atoms in the molecule along with the corresponding net atomic charge and point dipole moment components.

It may be observed from Table 1 that almost all of the electronegative atoms have acquired a negative charge except for the nitrogen atom at positions 8 and 15. The alkoxy carbon atoms have acquired partial positive charges and the hydrogen atoms attached to them carry partial negative charges. Ring carbon atoms have partial

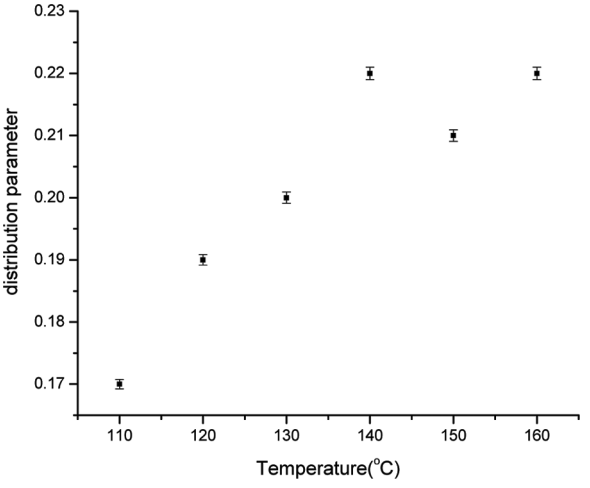

Figure 7. Variation of distribution parameter with temperature.

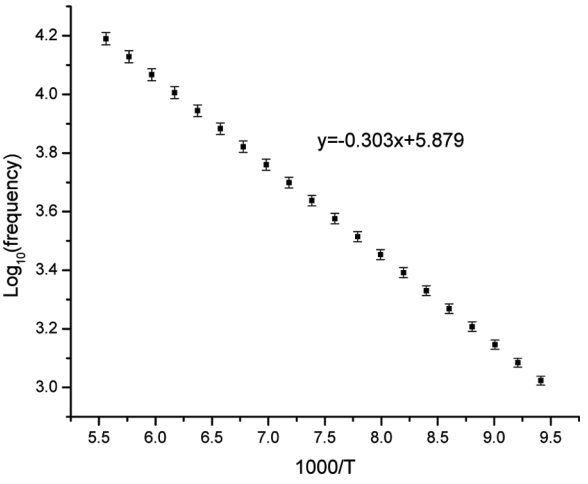

Figure 8. Variation of frequency ($\log_{10}$) with 10^3/T.

positive or negative charges depending on their position relative to the electronegative atom in the ring and the hydrogen atoms have opposite charges with respect to the carbon atoms holding them.

Table 2 shows the various types of energies associated with the molecule along with the calculated total dipole moment. Figures 10–12 display various minimum energy configurations obtained under different interacting conditions.

Table 3 summarizes the interaction energy values obtained for various configurations along with the contribution of each type of energy component. It should be noted here that the electrostatic terms, that is, monopole–monopole (E_{QQ}), monopole–dipole (E_{QM}), and dipole–dipole (E_{MM}) terms, determine the orientation of interaction because they are long-range interaction terms, whereas the rest of the terms contribute toward the stability of the association because they are short-range and largely depend on the extent of overlap between the interacting molecules.

Three stacking configurations 1, 2, and 3 are shown in Figure 10. Configuration 2 is the most preferred one with energy −46.88 kcal/mol and, as expected, shows a maximum overlap between the interacting molecules. Configuration 1 shows a better overlap of alkoxy tails but the energy is −37.6 kcal/mol. Configuration 3 shows a

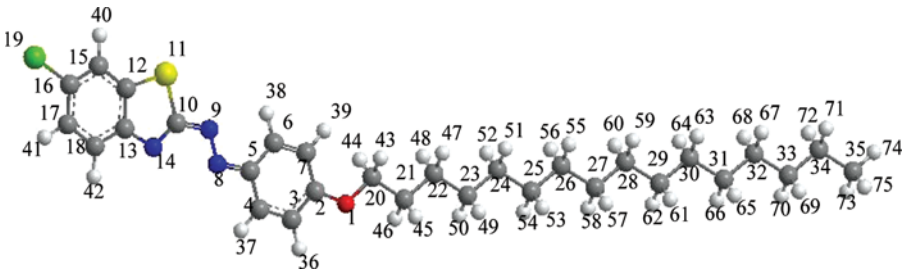

Figure 9. Numbering scheme of optimized geometry.

Table 1. Computed net atomic charges and point dipole moment components of 6CB4HPD at various atomic positions

Atom no.	Atom symbol	Optimized coordinate			Atomic charge	Point dipole moment components		
		X	Y	Z	q	μ_x	μ_y	μ_z
1	O	1.921135	1.250328	−0.20027	−0.76676	0.335963	0.088547	0.023886
2	C	3.015323	0.454379	−0.16258	0.396422	−0.38289	−0.09982	−0.02764
3	C	4.250011	1.119774	−0.05498	0.03659	0.001043	−0.18097	−0.00593
4	C	5.42378	0.389645	−0.00017	−0.51869	0.712159	0.261636	0.049292
5	C	5.398828	−1.01785	−0.05104	−0.10218	−1.16188	1.691578	−0.01111
6	C	4.160598	−1.6774	−0.16523	−0.14442	0.978001	−1.10305	0.024574
7	C	2.978888	−0.95342	−0.22178	0.059742	0.419421	−0.49782	0.013908
8	N	6.647533	−1.64654	0.024076	0.905641	−0.84781	−0.83201	−0.09661
9	N	6.610331	−2.91539	−0.01332	−0.19287	0.73907	−0.28172	0.047506
10	C	7.862718	−3.52433	0.071623	0.131767	0.47979	−1.54372	0.006868
11	S	7.795341	−5.30477	0.013484	−1.00802	−0.77739	−0.54598	−0.08707
12	C	9.5341	−5.31913	0.163852	−0.29018	−2.1695	−1.31795	−0.21091
13	C	10.00721	−3.97966	0.243948	0.817338	2.265248	−1.38256	0.155752
14	N	9.044283	−2.99823	0.189222	0.548999	−0.05273	−0.86019	−0.03456
15	C	10.40666	−6.40895	0.209478	−0.02307	2.00029	2.597554	0.22263
16	C	11.76365	−6.13401	0.336844	−0.62393	2.505146	−2.04908	0.165908
17	C	12.26137	−4.82097	0.418007	0.269841	−2.31948	0.077165	−0.20448
18	C	11.38716	−3.7458	0.371795	−1.44508	0.444163	1.085606	0.063506
19	Cl	12.89925	−7.47411	0.399598	−0.84371	0.662033	−0.81253	0.039544
20	C	0.619421	0.658422	−0.28163	1.155057	0.850711	−0.49336	−0.05015
21	C	−0.40494	1.782943	−0.23241	0.680261	0.335005	0.116135	0.048879
22	C	−1.84623	1.264488	−0.31813	0.587555	0.051708	−0.31628	−0.04958
23	C	−2.89364	2.380557	−0.21222	0.448335	0.106791	0.126047	0.017219
24	C	−4.33799	1.871309	−0.29673	0.370194	−0.06562	−0.12688	0.002764
25	C	−5.38711	2.981565	−0.15605	0.335913	0.096749	0.140518	−0.01485

26	C	−6.83218	2.472858	−0.23483	0.383961	−0.05123	−0.11981	0.020721
27	C	−7.88165	3.579943	−0.07345	0.32734	0.109321	0.151436	−0.02803
28	C	−9.32694	3.070768	−0.14481	0.390285	−0.04554	−0.11895	0.02782
29	C	−10.3763	4.176229	0.028128	0.328232	0.11099	0.152292	−0.03123
30	C	−11.8217	3.666366	−0.03565	0.390313	−0.04483	−0.11913	0.031287
31	C	−12.8708	4.771107	0.143042	0.345019	0.10185	0.159455	−0.02564
32	C	−14.3163	4.260539	0.086138	0.421704	−0.07479	−0.13246	0.028687
33	C	−15.3654	5.364734	0.266567	0.303533	0.08155	0.148479	−0.0248
34	C	−16.811	4.8539	0.215629	0.366896	−0.07174	−0.05232	0.027054
35	C	−17.8519	5.963651	0.395059	0.36055	−0.12078	0.082294	−0.03402
36	H	4.250996	2.203594	−0.01365	0.143497	0.014233	0.021663	0.001846
37	H	6.387969	0.879923	0.086467	0.015162	0.061968	0.047172	0.008066
38	H	4.148859	−2.76065	−0.20653	−0.18686	−0.11063	−0.18823	−0.01474
39	H	2.035411	−1.47831	−0.3107	0.057402	−0.01477	−0.06816	−0.00921
40	H	10.05299	−7.43153	0.149867	1.139116	0.100092	0.598635	0.034566
41	H	13.32911	−4.6621	0.516656	0.773344	−0.36698	−0.08443	−0.03148
42	H	11.74787	−2.72472	0.432752	0.14792	−0.02878	−0.03299	−0.00181
43	H	0.474803	−0.03583	0.557698	−0.32536	−0.0605	−0.15067	0.191808
44	H	0.530209	0.085351	−1.21523	−0.3619	−0.055	−0.13131	−0.23966
45	H	−0.26121	2.344817	0.698503	−0.26922	0.025373	0.131442	0.199983
46	H	−0.20361	2.479844	−1.05498	−0.25506	0.034296	0.155215	−0.17098
47	H	−2.02033	0.530855	0.481928	−0.27171	−0.04424	−0.14685	0.168212
48	H	−1.98668	0.72238	−1.26387	−0.28314	−0.03582	−0.11208	−0.20594
49	H	−2.75257	2.917748	0.736164	−0.20908	0.021097	0.094518	0.164129
50	H	−2.71986	3.119025	−1.00749	−0.19998	0.021984	0.122715	−0.12866
51	H	−4.5023	1.117016	0.486168	−0.1841	−0.02553	−0.11477	0.11847
52	H	−4.48475	1.350512	−1.2537	−0.18225	−0.01882	−0.08129	−0.14895
53	H	−5.23753	3.500968	0.801289	−0.17513	0.01792	0.0777	0.147639

(*Continued*)

Table 1. Continued

Atom no.	Atom symbol	Optimized coordinate			Atomic charge	Point dipole moment components		
		X	Y	Z	q	μ_x	μ_y	μ_z
54	H	−5.2245	3.737118	−0.93797	−0.1801	0.017083	0.113146	−0.1157
55	H	−6.98966	1.708891	0.540082	−0.18257	−0.02275	−0.11322	0.115334
56	H	−6.98612	1.963124	−1.19669	−0.17681	−0.01862	−0.07681	−0.14671
57	H	−7.72444	4.09036	0.887569	−0.1731	0.01706	0.074905	0.147799
58	H	−7.72678	4.343461	−0.84927	−0.18302	0.015356	0.114368	−0.11479
59	H	−9.47884	2.302999	0.627461	−0.18393	−0.02113	−0.11405	0.114987
60	H	−9.4869	2.565363	−1.10801	−0.17603	−0.01899	−0.07578	−0.14631
61	H	−10.2131	4.683329	0.989928	−0.17345	0.017258	0.074552	0.147983
62	H	−10.2272	4.942753	−0.74589	−0.18425	0.014663	0.114953	−0.11461
63	H	−11.9691	2.898066	0.736959	−0.18546	−0.02024	−0.11522	0.115519
64	H	−11.9865	3.161367	−0.99828	−0.17487	−0.01939	−0.07526	−0.14531
65	H	−12.7032	5.278155	1.104107	−0.18032	0.018997	0.076211	0.151393
66	H	−12.726	5.53787	−0.63156	−0.18786	0.015371	0.115535	−0.11633
67	H	−14.4603	3.493578	0.86076	−0.19663	−0.01926	−0.11925	0.121251
68	H	−14.4846	3.753631	−0.87491	−0.18625	−0.01933	−0.07781	−0.15164
69	H	−15.1957	5.874193	1.226147	−0.16444	0.017501	0.072653	0.141134
70	H	−15.2248	6.130519	−0.51	−0.17155	0.014337	0.108155	−0.10796
71	H	−16.9519	4.090624	0.993165	−0.15424	−0.0169	−0.1021	0.102379
72	H	−16.9806	4.343785	−0.74251	−0.15214	−0.01777	−0.0721	−0.13169
73	H	−17.761	6.722986	−0.3902	−0.13718	0.018939	0.107679	−0.10608
74	H	−18.872	5.567392	0.357259	−0.14869	−0.15707	−0.05733	0.000766
75	H	−17.7278	6.470884	1.358782	−0.12237	0.019605	0.067231	0.133763

Table 2. Computed total dipole moment with its components and electronic energy of 6CB4HPD molecule

Electronic energy (Hartree)	Dipole moment components			Total dipole moment (Debye)
−2227.06375549	−5.3745	1.9640	−0.2604	5.7281

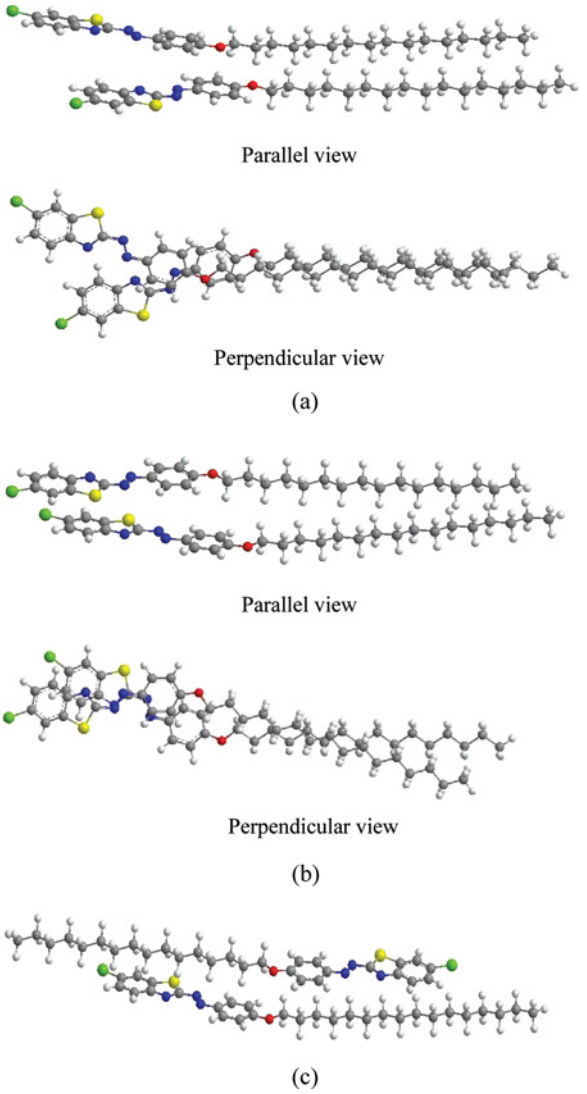

Figure 10. Minimum energy configuration for stacking interaction: (a) configuration 1 with total energy −37.5953 kcal/mol showing complete overlap of the alkoxy tail but less overlap of the benzothiazole ring; (b) configuration 2 with better overlap of the ring at the expense of reduced tail overlap (energy = −46.8807 kcal/mol); and (c) configuration 3 with total energy −35.1228 kcal/mole.

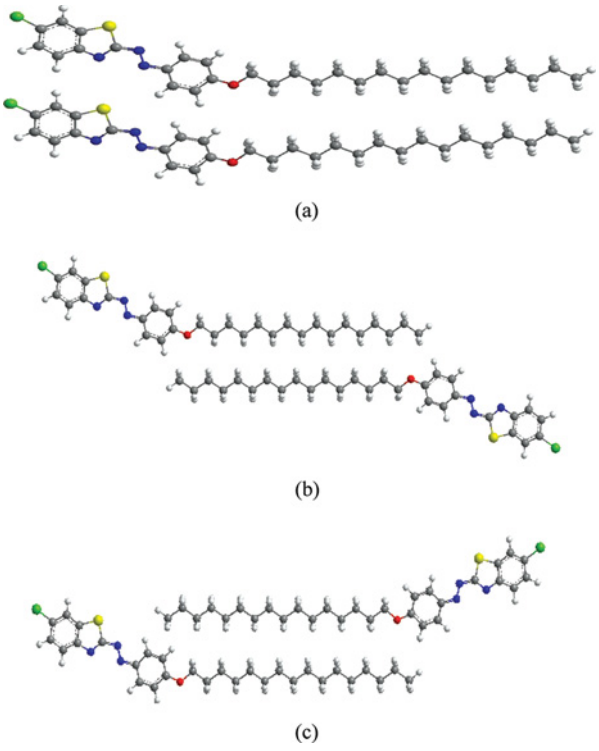

Figure 11. Minimum energy configuration for in-plane interaction: (a) configuration 4 with total energy −20.0554 kcal/mol; (b) configuration 5 with total energy −12.7494 kcal/mol; and (c) configuration 6 with total energy −18.8378 kcal/mol.

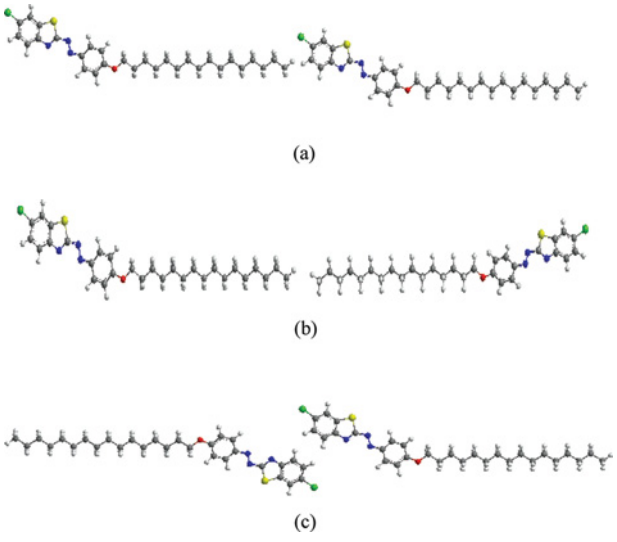

Figure 12. Minimum energy configuration for terminal interaction: (a) configuration 7 with total energy −2.0258 kcal/mol; (b) configuration 8 with total energy +0.4261 kcal/mol; and (c) configuration 9 with total energy −8.9843 kcal/mol.

Table 3. Intermolecular interaction energy in various configurations of stacking, in-plane, and terminal interactions

Energy component (kcal/mol)	Stacking interaction			In-plane interaction			Terminal interaction		
	Configuration 1	Configuration 2	Configuration 3	Configuration 4	Configuration 5	Configuration 6	Configuration 7	Configuration 8	Configuration 9
E_{QQ}	−0.9366	−3.4695	−1.5984	−13.6207	0.1513	1.4752	−2.4205	0.1520	−7.3725
E_{QM}	−12.8633	−20.6088	−8.2339	7.8917	−1.7329	−11.0205	3.4736	0.8616	−0.5855
E_{MM}	−0.9833	2.2531	0.2830	−2.1795	0.0375	−0.1380	−0.1090	−0.0082	1.2460
E_1	−14.7831	−21.8252	−9.5493	−7.9085	−1.5441	−9.6834	0.9441	1.0054	−6.7120
E_{POL}	−4.6682	−7.6979	−9.9150	−4.0917	−1.0100	−1.1754	−1.9240	−0.0160	−0.7886
E_{DISP}	−30.9858	−32.0204	−34.9971	−9.3306	−15.4561	−13.7328	−4.3427	−0.7413	−1.6798
E_2	−35.6539	−39.7201	−44.9121	−13.4233	−16.4662	−14.9082	−6.2667	−0.7573	−2.4683
E_{REP}	12.8418	14.6645	19.3385	1.2754	5.2608	5.7538	3.2968	0.1780	0.1960
$E_{TOTAL} = E_1 + E_2 + E_{REP}$	−37.5953	−46.8807	−35.1228	−20.0554	−12.7494	−18.8378	−2.0258	0.4261	−8.9843

head-to-tail type alignment although the interaction energy is −35.12 kcal/mol. Electrostatic interaction energy is also maximum for configuration 2, hence it may be concluded that at long range the most probable orientation for stacking is through configuration 2. Similar arguments on planar interactions show that although configuration 4 exhibits the lowest energy among the three possible modes of interaction, configuration 6 possesses the electrostatic minimum, hence, both configuration 4 and 6 are almost equally probable and configuration 5 is the least preferred one. Out of the three terminal interaction modes 7, 8, and 9, configuration 8 is repulsive and hence not likely to occur, whereas the electrostatic part of configuration 7 is repulsive, with total energy −2.03 kcal/mol, and thus has a poor binding capability. Configuration 9 interacts through a polar benzothiazole ring and possesses noticeable association energy −8.98 kcal/mol; hence it seems to be the most probable configuration. This is also supported by the fact that the compound has a high transition temperature (97°C) and thus the packing energy of the crystal must be very high.

The above discussion on intermolecular interaction between a molecular pair clearly suggests that the potential around each molecule is highly asymmetric in nature. The molecule has a strong tendency to form stacked layers along with an antiparallel planar link on both sides of the molecule. The terminal interactions are much weaker in comparison to stacking or in-plane interactions, although due to strong polar group at one end of the molecule, the molecule exists almost as a dimer unit, thus increasing the melting point of the crystal.

Conclusion

Dielectric properties and theoretical studies reported in this work clearly suggest that the potential around the 6CB4HPD molecules is highly asymmetric in nature. In the smectic range, the terminal association is almost broken. The molecule possesses a strong tendency to form a layered structure through stacking interactions, hence exhibiting a smectic phase. Planar interactions through configurations 4 and 6 are almost equivalent, although they correspond to flipping of the molecules. With the increase in temperature, the planar binding weakens and the molecules respond to higher frequencies better. Hence, the dielectric constant and loss curves shift toward higher frequency.

Acknowledgment

The authors are thankful to Dr. Devesh Kumar of the Molecular Modeling Group, I.I.C.T., Hyderabad, India, for helping in the computations. Computations facilities provided under the DST–FIST grant to the Department of Physics, D.D.U. Gorakhpur University, is also gratefully acknowledged.

References

[1] Bobadova-Parvanova, P., Parvanova, V., Petrov, M., & Tsonev, L. (2000). *Cryst. Res. Tech.*, *35*, 1321.
[2] Risser, S. M., & Ferris, K. F. (2002). *Mol. Cryst. Liq. Cryst.*, *373*, 143.
[3] Dunmur, D. A. (2005). *Liquid Crystals*, *32*, 1379.
[4] Morsy, M. A., Oweimreen, G. A., & Hwang, J. S. (1996). *J. Phys. Chem.*, *100*(20), 8331.

[5] Morsy, M. A., Oweimreen, G. A., & Al-Tawfiq, A. M. (1998). *J. Phys. Chem. B*, *102*, 3684.
[6] Kelly, S. M. (1996). *Liq. Cryst.*, *20*, 493.
[7] Born, M., & Oppenheimer, J. R. (1927). *Ann. Phys.*, *84*, 457.
[8] Pauling, L., & Wilson, E. B. (1935). *Introduction to Quantum Mechanics*, McGraw Hill: New York.
[9] Condon, E. U., & Shortley, G. H. (1935). *Theory of Atomic Spectra*, Cambridge University Press: London, UK.
[10] Schiff, L. I. (1968). *Quantum Mechanics*, 3rd ed., McGraw Hill: New York.
[11] Buckingham, A. D. (1978). *Intermolecular Interactios: From Diatomics to Biopolymers*. B. Pullman (Ed.), John Wiley & Sons: New York, 1.
[12] Claverie, P. (1978). *Intermolecular Interactions: From Diatomic to Biopolymers*. B. Pullman (Ed.), Wiley: New York, 69.
[13] Le Fevre, R. J. W. (1965). *Advances in Physical Organic Chemistry*, *3*, 1.
[14] Sanyal, N. K., & Ahmed, P. (1973). *J. Phys. Chem.*, *77*, 2552.
[15] Huron, M. J., & Claverie, P. (1969). *Chem. Phys. Lett.*, *4*, 429.
[16] Kitaigorodskii, A. I., Mirskaya, K. V., & Nauchitel, V. G. (1969). *Kritallographia*, *14*, 900.
[17] Huron, M. J., & Claverie, P. (1974). *J. Phys. Chem.*, *78*, 1862.
[18] Langlet, J., Claverie, P., Caron, F., and Bocuve, J. C. (1981). *Int. J. Quant. Chem.*, *20*, 299.
[19] Murrel, J. N., Kettle, S. F. A., & Tedder, J. M. (1965). *Valence Theory*, Wiley: London.
[20] Frisch, M. J., Trucks, G. W., Schlegel, H. B., Scuseria, G. E., Robb, M. A., Cheeseman, J. R., Montgomery, J. A. Jr., Vreven, T., Kudin, K. N., Burant, J. C., Millam, J. M., Iyengar, S. S., Tomasi, J., Barone, V., Mennucci, B., Cossi, M., Scalmani, G., Rega, N., Petersson, G. A., Nakatsuji, H., Hada, M., Ehara, M., Toyota, K., Fukuda, R., Hasegawa, J., Ishida, M., Nakajima, T., Honda, Y., Kitao, O., Nakai, H., Klene, M., Li, X., Knox, J. E., Hratchian, H. P., Cross, J. B., Bakken, V., Adamo, C., Jaramillo, J., Gomperts, R., Stratmann, R. E., Yazyev, O., Austin, A. J., Cammi, R., Pomelli, C., Ochterski, J. W., Ayala, P. Y., Morokuma, K., Voth, G. A., Salvador, P., Dannenberg, J. J., Zakrzewski, V. G., Dapprich, S., Daniels, A. D., Strain, M. C., Farkas, O., Malick, D. K., Rabuck, A. D., Raghavachari, K., Foresman, J. B., Ortiz, J. V., Cui, Q., Baboul, A. G., Clifford, S., Cioslowski, J., Stefanov, B. B., Liu, G., Liashenko, A., Piskorz, P., Komaromi, I., Martin, R. L., Fox, D. J., Keith, T., Al-Laham, M. A., Peng, C. Y., Nanayakkara, A., Challacombe, M., Gill, P. M. W., Johnson, B., Chen, W., Wong, M. W., Gonzalez, C., & Pople, J. A. (2004). *Gaussian 03, Rev. D. 01*, Gaussian, Inc: Wallingford, CT.
[21] Sanyal, N. K., Roychoudhury, M., Ojha, R. P., Shukla, S. R., & Ruhela, K. R. (1984). *Mol. Cryst. Liq. Cryst.*, *112*, 189.
[22] Roychoudhury, M., & Ojha, D. P. (1992). *Mol. Cryst. Liq. Cryst.*, *213*, 73.
[23] Ojha, D. P., Kumar, D., & Pisipati, V. G. K. M. (2002). (a) *Cryst. Res. Technol.*, *37*, 881; (b) (2002). *Z. Naturforch*, *57a*, 189; (c) (2002). *Mol. Cryst. Liq. Cryst.*, *378*, 65.